

**1 The influence of convection on the water isotopic**  
**2 composition of the TTL and tropical stratosphere**

D. S. Sayres<sup>1</sup>, L. Pfister<sup>2</sup>, T. F. Hanisco<sup>1,5</sup>, E. J. Moyer<sup>1,6</sup>, J. B. Smith<sup>1</sup>, J. M.

St. Clair<sup>1,4</sup>, A. S. OBrien<sup>1</sup>, M. Witinski<sup>1</sup>, M. Legg<sup>3</sup>, J. G. Anderson<sup>1</sup>,

---

D. S. Sayres, School of Engineering and Applied Sciences, Harvard University, 12 Oxford Street,  
Cambridge, MA 02138, USA. (sayres@huarp.harvard.edu)

<sup>1</sup>School of Engineering and Applied  
Sciences, Harvard University, 12 Oxford  
Street, Cambridge, Massachusetts, USA

<sup>2</sup>NASA Ames Research Center, Moffett  
Field, CA, USA

<sup>3</sup>BAERI, Sonoma, CA, USA

<sup>4</sup>now at Geology and Planetary Sciences  
Division, California Institute of Technology,  
Pasadena, CA

<sup>5</sup>now at NASA Goddard

<sup>6</sup>now at Department of Geophysical  
Sciences, University of Chicago, Chicago, IL

3 **Abstract.** We present the first in situ measurements of HDO across the  
4 tropical tropopause, obtained by the ICOS and Hoxotope water isotope in-  
5 struments during the CR-AVE and TC4 aircraft campaigns out of Costa Rica  
6 in winter and summer, respectively. We use these data to explore the role  
7 convection plays in delivering water to the tropical tropopause layer (TTL)  
8 and stratosphere. We find that isotopic ratios within the TTL are inconsis-  
9 tent with gradual ascent and dehydration by in-situ cirrus formation and sug-  
10 gest that convective ice lofting and evaporation play a strong role through-  
11 out the TTL. We use a convective influence model and a simple parameter-  
12 ized model of dehydration along back trajectories to demonstrate that the  
13 convective injection of isotopically heavy water can account for the predom-  
14 inant isotopic profile in the TTL. Although ice particles from convection at  
15 these altitudes were not directly observed during the flight campaigns, ob-  
16 servations include clear examples of residue of individual convective injec-  
17 tions of water vapor to near-tropopause altitudes. Air parcels with signifi-  
18 cantly enhanced water vapor and isotopic composition can be linked via tra-  
19 jectory analysis to specific convective events in the Western Tropical Pacific  
20 and Southern Pacific Ocean. The results suggest that deep convection is sig-  
21 nificant for the moisture budget of the tropical near-tropopause region and  
22 must be included to fully model the dynamics and chemistry of the TTL and  
23 lower stratosphere.

## 1. Introduction

24 Water vapor and ice exert a controlling influence on the radiative and dynamical bal-  
25 ance of the upper troposphere and lower stratosphere (UT/LS) and are key constituents  
26 in determining this region's response to climate forcing [*Smith et al.*, 2001; *Fasullo and*  
27 *Sun*, 2001; *Minschwaner and Dessler*, 2004]. The concentration of water vapor in the  
28 stratosphere also impacts the dosage of UV radiation reaching the surface through wa-  
29 ter's control of heterogeneous stratospheric ozone depletion [*Dvortsov and Solomon*, 2001;  
30 *Kirk-Davidoff et al.*, 1999]. In the UT/LS water vapor concentrations are central to the  
31 formation, evolution, and lifetime of cirrus that not only play a critical role in the radiative  
32 balance in the UT/LS but also in the dehydration of air ascending through the tropical  
33 tropopause layer (TTL). Changes in water vapor concentrations and the cirrus associated  
34 therewith control the radiative imbalance that amplifies climate forcing by CO<sub>2</sub> and CH<sub>4</sub>  
35 release at the surface and therefore quantifying the mechanisms that control water vapor  
36 in the TTL are key to predicting future changes in the climate system.

37 Quantifying the importance of convection in transporting boundary layer air to the  
38 TTL and lowermost stratosphere is pivotal for understanding the mechanisms that con-  
39 trol the stratospheric water vapor budget and accordingly that of other trace gases and  
40 particulates. Due to this importance much emphasis has been put on understanding the  
41 mechanisms that control the water vapor budget of the TTL and UT/LS. In general, wa-  
42 ter vapor in the TTL is removed by in-situ condensation and cirrus formation on cooling  
43 during ascent or advection through local cold regions [*Holton et al.*, 1995; *Holton and*  
44 *Gettelman*, 2001; *Fueglistaler et al.*, 2005]. Convection can however provide additional

45 sources of water via evaporation of convective ice in undersaturated TTL air [*Fu et al.*,  
46 2006; *Hanischo et al.*, 2007; *Dessler et al.*, 2007]. Distinguishing the relevant mechanisms  
47 will allow models to better simulate how water vapor pathways linking the troposphere  
48 and stratosphere will change with increased climate forcing by CO<sub>2</sub> and CH<sub>4</sub>. Many  
49 modeling studies that attempt to reproduce the observed water vapor mixing ratio of  
50 the TTL have suggested that convective ice lofting and evaporation may be unimportant  
51 to the region's water budget, and that mixing ratios of water vapor in air crossing the  
52 tropical tropopause can be well explained simply by the minimum temperature experi-  
53 enced by those air parcels [*Fueglistaler et al.*, 2004, 2005; *Gulstad and Isaksen*, 2007; *Cau*  
54 *et al.*, 2007]. However, attempts to simultaneously model HDO mixing ratios find that  
55 convection is necessary to accurately reproduce observed profiles of both H<sub>2</sub>O and HDO  
56 [*Dessler et al.*, 2007; *Bony et al.*, 2008]. Because water vapor isotopic composition is  
57 altered by all processes involving condensation or evaporation, the ratio of water vapor  
58 isotopologues (HDO/H<sub>2</sub>O or H<sub>2</sub><sup>18</sup>O/H<sub>2</sub>O) can act as a tracer of an air parcel's convective  
59 history [*Pollock et al.*, 1980; *Moyer et al.*, 1996; *Keith*, 2000]. Therefore, adding HDO  
60 to models constrains the amount of convection allowable in the model. Any model that  
61 attempts to explain the water vapor mixing ratio must also explain the water vapor iso-  
62 topologue ratio which is usually written as the ratio of the heavier isotope (e.g. HDO  
63 or H<sub>2</sub><sup>18</sup>O) to the more abundant lighter isotope (H<sub>2</sub>O) referenced to a standard. In the  
64 case of water the reference is the ratio in Vienna Standard Mean Ocean Water ( $R_{VSMOW}$ )  
65 [*Craig*, 1961a]. Deviations from the standard,  $\delta$ , are reported in permil (‰) where for the  
66 HDO/H<sub>2</sub>O ratio  $\delta D = 1000(HDO/H_2O/R_{VSMOW} - 1)$ . Values of  $\delta D \approx 0‰$  are found

67 close to the boundary layer and more negative values (e.g.  $\delta D = -600\text{‰}$ ) are found in  
68 highly dehydrated air masses near the tropopause.

69 Measurements of  $\delta D$  from canisters and remote observations have reported enriched  
70 values of HDO compared to what would be expected from simple thermally controlled  
71 dehydration mechanisms [*Moyer et al.*, 1996; *Johnson et al.*, 2001; *Kuang et al.*, 2003;  
72 *Ehhalt et al.*, 2005]. To try to better model the observed  $\delta D$  ratio *Dessler et al.* [2007],  
73 hereafter Dessler07, used the *Fueglistaler et al.* [2005] trajectory model and added a rep-  
74 resentation of convective ice flux to demonstrate that addition of water from evaporating  
75 convective ice was indeed a plausible explanation for isotopic enhancements observed by  
76 remote sensing instruments. Dessler07 was able to reproduce the  $\delta D$  profile from remote  
77 observations with only a small perturbation to the water vapor mixing ratio produced from  
78 the *Fueglistaler et al.* [2005] model. However, the lack of direct in situ observations of  $\delta D$   
79 in Dessler07 means that the parcel trajectories followed in the model can not be directly  
80 tied to the data which makes validation of the theory difficult. In addition, the range  
81 of  $\delta D$  observations used is sparse both spatially and temporally which makes regional,  
82 seasonal, and yearly variability not well quantified further complicating the comparison  
83 of the model to the remote observations.

84 In this paper we present the first in situ tropical measurements of HDO during both  
85 winter and summer. The high spatial and temporal resolution of the in situ data offer  
86 a more detailed test case than did the relatively coarse remote sensing data used in  
87 Dessler07. The in situ data are tied directly to diabatic back trajectories from the point  
88 of the measurement to identify sources of recent convective influence and to estimate the  
89 effect of convection on the  $\delta D$  ratio and the water vapor mixing ratio. We then use our own

90 convective influence scheme to evaluate whether a measurable difference in  $\delta D$  and water  
91 vapor mixing ratio is observed between data recently influenced by convection. Finally,  
92 as with Dessler07, we simulate the motion of air parcels along trajectories, tracking both  
93 water vapor and HDO in order to test if our model reproduces the profiles from the in situ  
94 data. However, we use real-time convection observations as opposed to the climatology  
95 of Dessler07.

## 2. Measurements

96 Isotopologue ratios were measured in situ aboard NASA's WB-57 high-altitude research  
97 aircraft during the Costa Rica Aura Validation Experiment (CR-AVE) in January and  
98 February, 2006 and the Tropical Composition, Cloud and Climate Coupling (TC4) cam-  
99 paign in August, 2007, both based out of Alajuela, Costa Rica, at  $9.9^\circ$  North latitude.  
100 Measurements of  $H_2O$ , HDO, and  $H_2^{18}O$  were obtained during these campaigns using  
101 the Harvard ICOS isotope instrument [Sayres *et al.*, 2009]. We focus here primarily on  
102 HDO which, although less abundant than  $H_2^{18}O$ , experiences stronger fractionation on  
103 condensation, giving isotope ratio observations more robustness against any instrument  
104 systematics. For TC4,  $H_2O$  and HDO measurements were also obtained by the total water  
105 Hoxotope instrument [St. Clair *et al.*, 2008]. Water vapor mixing ratios are reported us-  
106 ing the Harvard Lyman- $\alpha$  hygrometer [Weinstock *et al.*, 1994], which has a long heritage  
107 on the WB-57 aircraft.

108 Data reported here are screened for both potential contamination and potential in-  
109 strument systematics. To preclude inclusion of any ICOS data subject to contamination  
110 from water desorbing off the instrument walls, we report only ICOS data where ICOS  
111 water vapor is less than 0.5 ppmv greater than that reported by Harvard Lyman- $\alpha$ . The

112 Hoxotope instrument uses the technique of photofragment fluorescence and therefore is  
113 far less subject to wall contamination. An additional potential source of measurement  
114 uncertainty in the ICOS data is optical fringing and other artifacts in the baseline power  
115 curve, which can produce measurement biases that manifest themselves as offsets in mea-  
116 sured  $\delta D$ . While fitting routines developed for ICOS (as described in *Sayres et al.* [2009])  
117 mitigate some potential sources of bias, residual offsets on the order of 50‰ to 100‰ are  
118 still occasionally present. Periods of high potential bias are however readily identified and  
119 for this work we have removed all data with potential biases greater than the short term  
120  $1-\sigma$  measurement precision. Quality-controlled ICOS data during CR-AVE in the driest,  
121 most signal-limited conditions ( $H_2O < 10$  ppmv) show a maximum uncertainty in  $\delta D$  of  
122 30‰ (10 sec.,  $1-\sigma$ ). (In wetter air, signal to noise is higher and therefore isotopic ratio  
123 uncertainty lower). For the TC4 mission, a laser change in the ICOS instrument resulted  
124 in increased bias uncertainty in low-signal conditions. We therefore show here ICOS data  
125 from TC4 only for wetter conditions ( $H_2O > 10$  ppmv) and use Hoxotope data for dry  
126 conditions or for flights when ICOS did not report data. The base Hoxotope precision  
127 is 85‰ (10 sec.,  $1 \sigma$ ). Although these uncertainties exceed those of laboratory-based  
128 mass spectrometers, they represent the most sensitive in situ water isotope measurements  
129 made in these conditions, and are comparable with the performance of remote sensing  
130 instruments while providing far higher spatial and temporal resolution.

131 In order to restrict our analysis to true tropical airmasses we show here only data from  
132 tropical flight segments out of Alajuela, Costa Rica in which the WB-57 aircraft made  
133 vertical transects through the tropopause while in the deep tropics, i.e. at latitudes below  
134  $10^\circ$  North. Flights with segments meeting both the geographic and data quality criteria

135 in the wintertime (CR-AVE) campaign occurred on January 30, and February 1, 2, and  
136 7, 2006; in the summertime (TC4) campaign on August 6, 8, and 9, 2007 (Hoxotope) and  
137 August 8 and 9, 2007 (ICOS). We include water vapor data from the Lyman- $\alpha$  instrument  
138 for all these flight legs and in addition for the qualifying flight of August 5, 2007, during  
139 which no isotopic data was available.

### 3. Mean tropical $\delta D$ profiles

140 The isotopic composition of water vapor in the tropical atmosphere shows a sharp  
141 distinction in behavior between the bulk of the troposphere and the TTL (Figure 1).  
142 Below the TTL, both water vapor and  $\delta D$  fall off with altitude much as expected in pure  
143 Rayleigh distillation, where preferential removal of heavier condensate leaves the residual  
144 vapor progressively lighter [Jouzel *et al.*, 1985; Ehhalt *et al.*, 2005]. In the TTL water  
145 vapor concentrations continue to decrease to the tropopause while isotopic composition  
146 remains roughly constant. This feature is persistent in both summertime and wintertime  
147 observations, but some seasonal difference is evident. The TTL is isotopically lighter  
148 in the wintertime CR-AVE data with a mean  $\delta D$  of -650‰, and shows a discontinuity  
149 starting at 370 K to isotopically heavier air with a mean of -500‰. This shift is not well  
150 correlated with the slight increase in the water vapor measurements above the tropopause  
151 as the shift in  $\delta D$  starts below the tropical tropopause. In the stratosphere proper, the  
152  $\delta D$  measurements are invariant within the precision limits of the data, while the water  
153 vapor mixing ratio increases linearly. In the summertime TC4 data, with nearby ITCZ  
154 convection, the TTL is isotopically heavier with a mean  $\delta D$  of -550‰ and its composition  
155 is continuous with the stratosphere proper. All these results suggest that evaporation of  
156 convective ice is a significant factor in affecting the isotopic composition of TTL water

157 in both the summertime and wintertime. While in both campaigns the WB-57 did not  
158 directly intercept convective outflow at the top of the TTL or stratosphere, evidence of  
159 evaporation of convective ice is found in the summertime data which show two plumes  
160 of enhanced water vapor at 390 and 405 K and a second profile between 390 and 420 K  
161 that is 0.5 ppmv wetter than the mean profile (denoted by arrows in Figure 1). The two  
162 plumes were sampled during August 5th when no isotope data are available.

163 The observed tropical TTL isotopic profile is incompatible with simple dehydration dur-  
164 ing gradual ascent, which would produce isotopic depletion along with dehydration. In the  
165 bulk of the troposphere, from the lowest observations to the base of the TTL ( $\theta = 355$ - $360$   
166 K), observed water isotopic composition is roughly consistent with Rayleigh distillation.  
167 Water vapor concentrations fall by over two orders of magnitude and isotopic composi-  
168 tion drops to approximately  $-700\%$ . Within the TTL, however, observed near-constant  
169 isotopic composition cannot be explained by a simple Rayleigh distillation model. (Model  
170 calculations are shown for comparison in Figure 1, in gray, with the range representing  
171 condensate retention between 0 and 80%). Gradual ascent and pure Rayleigh distillation  
172 within the TTL would have further reduced vapor isotopic composition to some  $-900\%$ .  
173 In the stratosphere proper, we would expect no further change save a slight increase due  
174 to methane oxidation as air ages. To within the precision of the data,  $\delta D$  is indeed invari-  
175 ant above the tropopause; the aircraft flights do not sample high enough altitudes or old  
176 enough air ages for methane oxidation to be significant.

177 Thus far we have evaluated the water vapor and  $\delta D$  measurements separately even  
178 though when in equilibrium they follow a very tight relationship that can be seen by  
179 plotting the logarithm of the water vapor mixing ratio versus  $\delta D$  (Figure 2). As in Figure

180 1 the data are isotopically heavy compared to a simple Rayleigh model. The Rayleigh  
181 relationship modeled here assumes that the air parcels sampled followed a single Rayleigh  
182 distillation curve given by the temperature profile measured by the WB-57 out of Costa  
183 Rica. Even if this temperature profile is representative of the tropics, ice evaporation in the  
184 free troposphere or lower part of the TTL would have the effect of shifting the Rayleigh  
185 curve. As an example, if the Rayleigh curve is shifted by 200‰ below the TTL, the  
186 subsequent relationship between water vapor and  $\delta D$  would follow the light-gray shaded  
187 region shown in Figure 2. The CR-AVE data and most of the TC4 data greater than  
188 10 ppmv water vapor fall on this shifted curve indicating that convection at or below  
189 the base of the TTL is important for setting the  $\delta D$  value at the base of the TTL. The  
190 enrichment at the base of the TTL therefore may be due to convective ice evaporation  
191 in the mid-troposphere, more likely in summertime. In the wintertime that enrichment  
192 may have taken place in a different part of the tropics or perhaps even reflect an influx  
193 of midlatitude air [*Hanisco et al.*, 2007; *James and Legras*, 2009]. However, below water  
194 vapor mixing ratios of 10 ppmv, corresponding to the upper TTL and lower stratosphere  
195 the simple relationship between water vapor and  $\delta D$  is no longer valid. This implies that  
196 convective enhancements lower in the troposphere can only explain the data up to the  
197 middle of the TTL. To account for the enriched water vapor sampled at the top of the  
198 TTL and lower stratosphere, convection must reach the top of the TTL.

199 One other possible mechanism that would shift the Rayleigh curve is ice formation  
200 under supersaturated conditions. When ice forms under these conditions, kinetic effects  
201 between the isotopologues dominate over the thermodynamics with the result that  $\delta D$  is

202 shifted to less depleted values as shown in Figure 1 by the solid and dashed black lines  
203 representing condensation at 120% and 150% relative humidity over ice.

204 Whether condensation at high supersaturation is a major factor in determining the  $\delta D$   
205 ratio can be evaluated by looking at the relationship between  $\delta D$  and  $\delta^{18}O$ . If condensation  
206 follows a Rayleigh process (i.e. is in thermodynamic equilibrium) then the slope of the  $\delta D$   
207 to  $\delta^{18}O$  relationship follows the well known meteoric water line (MWL) (Figure 3, thick  
208 black curved line) [*Craig, 1961b*]. As the level of supersaturation increases, the heavier  
209  $H_2^{18}O$  isotopologue is less depleted relative to HDO resulting in the slope between  $\delta D$  and  
210  $\delta^{18}O$  becoming shallower as shown by the dashed lines in Figure 3. Data falling below  
211 the MWL can occur from mixing between parcels with  $\delta$  ratios at different points along  
212 the MWL. Data from CR-AVE and TC4 are plotted in blue and cyan respectively and lie  
213 either on the MWL or below in the mixed region. We therefore conclude that condensation  
214 at high supersaturation is not a major factor controlling the shift in  $\delta D$  away from the  
215 Rayleigh curve and leaves convective ice lofting and subsequent evaporation as the sole  
216 possible mechanism for the observed enhancements in  $\delta D$ .

217 To confirm the implication that convection within the TTL is a source of isotopic  
218 enhancement, we conduct two modeling studies. First, we use a back-trajectory model  
219 and maps of past convection to examine the isotopic impact of convection. Second, we  
220 model isotopic evolution along those trajectories to verify that addition of convective ice  
221 can produce the observed enhancements.

#### 4. Back Trajectories and Convective Influence Model

222 The high spatial and temporal resolution of the in situ data allow us to use back trajec-  
223 tories to determine which sampled air parcels have been influenced by recent convective

224 events and evaluate whether convective influence is indeed correlated with isotopic en-  
225 hancement. We use for this purpose an analysis framework similar to *Pfister et al.* [2001]  
226 and briefly documented in *Pfister et al.* [2009, this issue]. Diabatic back-trajectories  
227 (BTs) are performed along the flight tracks of the WB-57 aircraft using the GSFC trajec-  
228 tory model [*Schoeberl and Sparling, 1995*] driven by the GEOS-4 analysis [*Bloom et al.,*  
229 2005] and radiative heating rates. For the TC4 calculations, we used the mean July clear-  
230 sky radiative heating rates from *Rosenfeld* [1991]. For CR-AVE, we used mean winter  
231 all-sky heating rates calculated by *Yang et al.* [2009]. For each aircraft point, a cluster of  
232 14 day BTs are calculated in order to minimize errors from the BTs and also to allow for  
233 a gradient in convective influence, as the convective systems in the TTL are narrow and  
234 scarce. Each cluster has 15 points at 3 altitudes; 0.5 km above the aircraft level, at the  
235 aircraft level, and 0.5 km below the aircraft level. At each level there are 5 points along  
236 a line perpendicular to the aircraft flight track, each separated by 0.3 degrees. The BTs  
237 are run along theta surfaces, with the parcels moving across theta surfaces as indicated  
238 by the GEOS-4 heating rates. To calculate convective influence, the BTs are run through  
239 a time varying field of satellite brightness temperature, using global geostationary, 8 km  
240 resolution, 3 hourly satellite imagery. Convective influence is defined as occurrences along  
241 the BTs where the satellite brightness temperature is less than or equal to the trajectory  
242 temperature. Convective encounters are allowed even if the trajectory is as much as 0.25  
243 degrees distant from the cold temperature.

244 The CR-AVE trajectories (Figure 4, plots *A* and *C*) show a clear separation in the  
245 origin of the air near the tropopause. Air from the free troposphere and throughout  
246 the TTL up to 390 K originates in the Western Tropical Pacific (WTP) and Southern

247 Pacific Ocean. Air above 390 K mostly originates from over the Caribbean or has been  
248 sitting over the northern part of South America for much of the 14 day trajectories. A few  
249 trajectories also follow the tropospheric air that originates from the Southern Pacific. The  
250 trajectories from TC4 (plot *B* and *D*) are more uniform with air throughout the TTL and  
251 stratosphere originating either from the Asian monsoon region moving westward or from  
252 the southern Pacific Ocean and moving eastward. This is also consistent with the uniform  
253  $\delta D$  measurements made during TC4. The model indicates that convective events reach as  
254 high as 410 K in the WTP and over South America during TC4. During CR-AVE deep  
255 convection occurs over South America and the Southern Pacific Ocean. Both patterns are  
256 consistent with observed isotopic profiles, with a sharper discontinuity in tropopause  $\delta D$   
257 during CR-AVE and more uniform  $\delta D$  measurements during TC4.

258 The convective influence model, however, only indicated the possibility that convection  
259 has influenced the water vapor mixing ratio, as the amount of detrained ice that can  
260 evaporate depends on the level of saturation of the ambient air. For the convection to affect  
261 the water vapor mixing ratio we add a constraint to the model that requires the mixing  
262 ratio of water vapor to be below the saturation mixing ratio calculated along the trajectory  
263 at the point of potential convective influence. Only if this criteria is met can convection  
264 meaningfully moisten the air parcel. We attempt to identify such undersaturated parcels  
265 by constructing a pseudo- relative humidity using measured water vapor along the flight  
266 track and pressure and temperature along the back-trajectory. For example, the convective  
267 events over the Southern Pacific Ocean during CR-AVE reach up to 405 K (Figure 4, plot  
268 *C*) and the air during this time is undersaturated compared with the measured water  
269 vapor mixing ratio with pseudo relative humidity below 60% (Figure 4, plot *E*). These

270 convective events would be expected to hydrate the air parcels with evaporated ice. The  
271 convective events over South America that reach up to 410 K but occur when the air  
272 parcels are near saturation are less likely to influence the water vapor mixing ratio as the  
273 ice particles will likely fall before evaporating.

274 This protocol has one obvious weakness, that we cannot discriminate between humidity  
275 that pre-dates convective influence and that derived from convection itself. A parcel with  
276 100% relative humidity at the point of convection may have been saturated beforehand,  
277 and therefore experienced no convective influence, or it may have become saturated from  
278 evaporating ice, and therefore experienced maximum convective influence. However, in  
279 the atmosphere we do not expect convective ice evaporation to bring parcels completely  
280 to saturation, and in this case the pseudo-relative humidity test remains meaningful.  
281 Furthermore, even a small change in water content can produce a large change in isotopic  
282 composition. We therefore define our complete convective influence criterion as that more  
283 than 50% of cluster BTs intersect convection (as defined above) and that pseudo-relative  
284 humidity at the point of intersection is less than 80%.

285 Both the summertime (TC4) and wintertime (CR-AVE) data show convective influence  
286 throughout the TTL and into the lower tropical stratosphere, with summertime convec-  
287 tion extending higher than wintertime (Figure 5). Though convection was not directly  
288 measured above the base of the TTL during TC4 or CR-AVE, there is clear observational  
289 evidence of convection penetrating above 400 K in the tropics. *Kelly et al.* [1993] and  
290 *Pfister et al.* [1993] noted hydration associated with convection up to 410 K in northern  
291 Australia. More recently, *Corti et al.* [2008] have noted hydration up to 420 K, both in  
292 Australia and South America. As noted earlier, the data presented here show residual

293 evidence of convection indicated by the water vapor measurements shown in Figure 5  
294 where between 390 K and 420 K there are two distinct profiles which differ by 0.5 ppmv  
295 water vapor, the wetter profiles being labeled as air parcels that have been recently in-  
296 fluenced by convection. While not all wet points coincide with convectively influenced  
297 points, trajectories beyond seven days are not accurate enough to correctly identify spe-  
298 cific convective events. Even with this uncertainty, the trajectories still have statistical  
299 validity. We would expect to see some convective influence in data taken over several  
300 flight days where the model indicates overall convective influence over the same flights in  
301 the same area. The 14 day time period is also significant because the back trajectories do  
302 not always reach the Asian monsoon region in that time (TC4), or the deepest convection  
303 in the Western Pacific (CR-AVE).

304 With the definitions for positive influence of convection on the water vapor mixing  
305 ratio defined above, we find that during the summertime a larger percentage of the data  
306 within the last 14 days has been influenced by convection. During the wintertime 37%  
307 of the data were influenced by convection within the TTL with a sharp cut off around  
308 390 K. During the summertime 56% of the data samples were influenced by convection  
309 within the TTL and 37% of data samples were influenced by convection above 390 K.  
310 The highest potential temperatures that convective influence was observed at was 388 K  
311 and 414 K during winter and summer, respectively. Both convective events occurred over  
312 South America.

313 The convective influence calculations do not themselves show that convection can influ-  
314 ence the isotopic composition of TTL water, as within the precision of the measurements,  
315 the  $\delta D$  data within the TTL do not show a quantitative separation between data that

316 is identified as with or without convective influence. (Above 380 K, the convectively in-  
317 fluenced data for the  $\delta D$  measurements tend to lie to the heavier side of the measured  
318 prole, though this difference is within the uncertainty of the measurements). This lack  
319 of discrimination is likely due to mixing during the 14 day trajectories and error in back  
320 trajectories. The model results do however highlight the extent of convection within the  
321 TTL and lower stratosphere.

## 5. Isotope Simulation

322 To help establish whether evaporating convective ice can indeed explain the observed  
323 non-Rayleigh isotopic profiles in the tropical TTL, we have added a simulation of isotopic  
324 evolution to the back-trajectories and convective influence model described above. We  
325 use a Rayleigh model and NCEP reanalysis temperatures to provide initial water vapor  
326 and HDO concentrations for the start of each trajectory assuming that the initial wa-  
327 ter vapor mixing ratio is equal to the saturation mixing ratio. We run two cases of  $\delta D$   
328 assumptions, the first assuming a start value set by simple Rayleigh distillation and the  
329 second an initial value enhanced by 200‰, reflecting the observed tropospheric enhance-  
330 ments. Temperature and relative humidity are then calculated along the trajectory. As  
331 the trajectory is run forward, if the air parcel cools the relative humidity is kept equal  
332 to 100% and it is assumed that any removal of water by condensation follows Rayleigh  
333 distillation and this provides the resultant  $\delta D$ . If the temperature increases and the air  
334 becomes undersaturated then the concentrations of H<sub>2</sub>O and HDO are left constant unless  
335 there is convective influence. If there is convective influence the model hydrates the air to  
336 saturation with evaporated ice that has a  $\delta D$  of -100‰ (see ice data highlighted in Figure  
337 1 and *Hanisco et al.* [2007])

338 The results of this simple model, using trajectories from TC4 that start between 350 and  
339 360 K, suggest that observed convection over just 14 days can produce significant isotopic  
340 enhancement in the TTL (Figure 6, with trajectories that were influenced by convection  
341 plotted in red). Most trajectories ascend to their final potential temperature of between  
342 370 and 390 K in 14 days. During that time water vapor decreases to between 3 and 7  
343 ppmv. Convective enhancements of water vapor and HDO occurred throughout the TTL  
344 with events above 370 K being more pronounced in both water vapor and  $\delta D$ . However, by  
345 the time the trajectories reach the top of the TTL or lower stratosphere (where they would  
346 be sampled by the WB-57) the enhanced water vapor signature has been mostly washed  
347 out by desiccation in the model; though in the atmosphere it can also be washed out by  
348 mixing. The exception is the event at 385 K in which water vapor remains high (8 ppmv)  
349 since this event occurred above the tropopause and did experience further cooling. On  
350 the other hand, the  $\delta D$  signature is very distinct as the amount of subsequent depletion is  
351 small since only a few ppmv of water vapor is removed. The difference between trajectories  
352 that encountered convection and those that did not is between 200‰ and 300‰ (Figure 6,  
353 plot *A*). Convection at the base of the TTL does not greatly affect the final mean value of  
354  $\delta D$  for the profiles that have subsequent convective influence (red profiles in plots *A* and  
355 *B*). However, for the profiles that are not otherwise convectively influenced (blue profiles),  
356 a shift of 200‰ at the start of the trajectory produces a shift ranging from 0‰ to 200‰  
357 in the final  $\delta D$  value, with the result that the mean  $\delta D$  value has been shifted by 150‰  
358 and the spread of values broadened (Figure 6, plot *B*). This makes the separation in  $\delta D$   
359 between the parcels that were influenced by convection in the TTL and those that were  
360 not much smaller. This is consistent with the in situ data that show little difference in

361  $\delta D$  between data marked as being convectively influenced in the TTL. Since the model  
362 only starts at the beginning of the 14 trajectories, it will not account for convection that  
363 occurred prior to this period. In addition, the absence of mixing and diffusion in the model  
364 tends to enhance the differences between convectively and non-convectively influenced air.  
365 All these limitations in the simulation and model will tend to make the separation between  
366 convectively and non-convectively influenced data greater in the simulation as compared  
367 to the actual in situ data.

## 6. Conclusions

368 We present the first in situ measurements of  $\delta D$  in the tropics during summertime and  
369 wintertime. This represents a unique data set to test models of dehydration in the TTL.  
370 In situ profiles of  $\delta D$  measured in the tropics during both summertime and wintertime  
371 show enrichment compared to the expected value if water vapor mixing ratio is controlled  
372 solely by minimum temperature. The wintertime measurements have a minimum  $\delta D$  of  
373  $-650\text{‰}$  at the base of the TTL and are then constant up to 370 K. At the top of the  
374 TTL and through the lower tropical stratosphere there is a increase in  $\delta D$  to  $-500\text{‰}$   
375 accompanied by a small increase in water vapor mixing ratio. The summertime data  
376 show enriched air starting at the base of the TTL and a uniform  $\delta D$  value throughout  
377 the TTL and stratosphere with a mean  $\delta D$  of  $-550\text{‰}$ . Water vapor data show plumes of  
378 high water at 390 and 405 K and two distinct profiles between 390 and 420 K, with the  
379 wetter profile having a water vapor mixing ratio 0.5 ppmv higher than the dry profile.  
380 The data presented here are consistent with the conclusions of Dessler07 and indicate that  
381 convection moistens the TTL and is required to explain the enriched  $\delta D$  measurements.

382 Back-trajectory analysis for the CR-AVE and TC4 data shows that the isotopic dis-  
383 continuity at the tropopause in the wintertime CR-AVE data is likely real and reflects a  
384 different origin for air in TTL and stratosphere. It also supports the conclusion that was  
385 also drawn qualitatively from the tropical isotopic profiles that potential convective influ-  
386 ence occurs throughout the TTL. The back-trajectory analysis is able to tie air parcels  
387 back to specific convective events. The back trajectories from CR-AVE and a convective  
388 influence model show the enrichment in both HDO and water vapor above 370 K comes  
389 from convection over the southern Pacific Ocean ( $\approx 20^\circ\text{S}$ ). There is also strong convection  
390 over South America, but as the air is likely saturated during the time of the convection  
391 the effect on water vapor is presumably small. The back trajectories from TC4 show air  
392 parcels linked to deep convection up to 414 K throughout the Western Tropical Pacific  
393 and a few events over South America with the air in both regions being likely unsatu-  
394 rated. The convective influence model identifies the majority of samples from the high  
395 water vapor profile as being convectively influenced in the previous 14 days.

396 The  $\delta\text{D}$  data within the TTL do not show a quantitative separation between data that  
397 is identified as being convectively influenced within the precision of the measurements.  
398 This is in agreement with all data being convectively influenced at the base of the TTL  
399 or before the 14 days of the trajectory. Above 380 K, the convectively influenced data for  
400 the  $\delta\text{D}$  measurements tend to lie to the heavier side of the measured profile, though this  
401 difference is within the uncertainty of the measurements. The combination of isotopically  
402 enriched air throughout the TTL even as water vapor decreases, the evidence of frequent  
403 convective events reaching these particular airmasses, and demonstration that convective  
404 ice evaporation can produce the isotopic enhancements seen, all suggest strongly that

405 the dominant process governing the observed isotopic profiles in the TTL is addition of  
406 convective ice. In order to observe this convective effect predicted by the model more  
407 directly, and to quantify the  $\delta D$  of ice injected into the TTL, measurements should be  
408 made closer to the sources of convection. Based on the back trajectory model this would  
409 be the Western Tropical Pacific and the southern Pacific Ocean.

410 Both the convective influence scheme and the  $\delta D$  and water vapor measurements show  
411 that convection reaches as high as 414 K in the tropics during summertime. As these  
412 enhancements in water vapor mixing ratio occur above the local tropopause it is likely  
413 that these air parcels will not be further dehydrated and that convection has permanently  
414 moistened the tropical stratosphere. Though convective events at altitudes above the  
415 tropical tropopause are scarce, these events nevertheless moisten the tropical stratosphere.  
416 The importance of this process for the global stratospheric water budget is still not clear  
417 due to the small sample size as well as the possibility of large yearly variability. In addition  
418 to ice and water vapor, deep convection also may bring into the UT/LS other trace gas  
419 species and particulates that can have an effect on ozone chemistry and cloud formation.

420 Including deep convection in global climate models will be important for predicting  
421 the effect of changes in temperature on the climate system. The data clearly show, as  
422 Dessler07 and others have also suggested, that to correctly estimate the global amount  
423 of water vapor that crossed the tropical tropopause convection must be included. To  
424 quantify the water vapor added by deep convection more measurements will be necessary  
425 in the tropics particularly in the areas that the convective influence model indicated as  
426 being convectively active.

<sup>427</sup> **Acknowledgments.** The authors wish to thank the WB-57 pilots and crew for  
<sup>428</sup> their hard work and dedication without which these measurements would not be pos-  
<sup>429</sup> sible. We also gratefully acknowledge the support of NASA grants NNG05G056G and  
<sup>430</sup> NNG05GJ81G.

## References

- 431 Bloom, S., A. da Silva, D. Dee, M. Bosilovich, J. Chern, S. Pawson, S. Schubert,  
432 M. Sienkiewicz, I. Stajner, W. Tan, and M. Wu (2005), Documentation and valida-  
433 tion of the goddard earth observing system (geos) data assimilation system - version 4  
434 . technical report series on global modeling and data assimilation, *Document 104606*,  
435 *26*, NASA.
- 436 Bony, S., C. Risi, and F. Vimeux (2008), Influence of convective processes on the iso-  
437 topic composition ( $\delta$  O-18 and  $\delta$  D) of precipitation and water vapor in the  
438 tropics: 1. Radiative-convective equilibrium and Tropical Ocean-Global Atmosphere-  
439 Coupled Ocean-Atmosphere Response Experiment (TOGA-COARE) simulations, *Jour-*  
440 *nal of Geophysical Research-Atmospheres*, *113*(D19), doi:10.1029/2008JD009942.
- 441 Cau, P., J. Methven, and B. Hoskins (2007), Origins of dry air in the tropics and sub-  
442 tropics, *Journal of Climate*, *20*(12), 2745–2759, doi:10.1175/JCLI4176.1.
- 443 Corti, T., B. P. Luo, M. de Reus, D. Brunner, F. Cairo, M. J. Mahoney, G. Martucci,  
444 R. Matthey, V. Mitev, F. H. dos Santos, C. Schiller, G. Shur, N. M. Sitnikov, N. Spelten,  
445 H. J. Vossing, S. Borrmann, and T. Peter (2008), Unprecedented evidence for deep  
446 convection hydrating the tropical stratosphere, *Geophysical Research Letters*, *35*.
- 447 Craig, H. (1961a), Standard for reporting concentrations of deuterium and oxygen-18 in  
448 natural waters, *Science*, *133*, 1833–&.
- 449 Craig, H. (1961b), Isotopic variations in meteoric waters, *Science*, *133*, 1702–&.
- 450 Dessler, A. E., T. F. Hanisco, and S. Fueglistaler (2007), Effects of convective ice lofting  
451 on h<sub>2</sub>o and hdo in the tropical tropopause layer, *Journal Of Geophysical Research-*  
452 *Atmospheres*, *112*.

- 453 Dvortsov, V. L., and S. Solomon (2001), Response of the stratospheric temperatures and  
454 ozone to past and future increases in stratospheric humidity, *Journal Of Geophysical*  
455 *Research-Atmospheres*, *106*, 7505–7514.
- 456 Ehhalt, D., F. Rohrer, and A. Fried (2005), Vertical profiles of HDO/H<sub>2</sub>O in the tropo-  
457 sphere, *Journal of Geophysical Research-Atmospheres*, *110*(D13).
- 458 Fasullo, J., and D. Z. Sun (2001), Radiative sensitivity to water vapor under all-sky  
459 conditions, *Journal Of Climate*, *14*, 2798–2807.
- 460 Fu, R., Y. L. Hu, J. S. Wright, J. H. Jiang, R. E. Dickinson, M. X. Chen, M. Filipiak,  
461 W. G. Read, J. W. Waters, and D. L. Wu (2006), Short circuit of water vapor and  
462 polluted air to the global stratosphere by convective transport over the tibetan plateau,  
463 *Proceedings Of The National Academy Of Sciences Of The United States Of America*,  
464 *103*, 5664–5669.
- 465 Fueglistaler, S., H. Wernli, and T. Peter (2004), Tropical troposphere-to-stratosphere  
466 transport inferred from trajectory calculations, *Journal Of Geophysical Research-*  
467 *Atmospheres*, *109*.
- 468 Fueglistaler, S., M. Bonazzola, P. H. Haynes, and T. Peter (2005), Stratospheric water  
469 vapor predicted from the lagrangian temperature history of air entering the stratosphere  
470 in the tropics, *Journal Of Geophysical Research-Atmospheres*, *110*.
- 471 Gulstad, L., and I. S. A. Isaksen (2007), Modeling water vapor in the upper troposphere  
472 and lower stratosphere, *Terrestrial Atmospheric and Oceanic Sciences*, *18*(3), 415–436,  
473 doi:10.3319/TAO.2007.18.3.415.
- 474 Hanisco, T. F., E. J. Moyer, E. M. Weinstock, J. M. St Clair, D. S. Sayres, J. B. Smith,  
475 R. Lockwood, J. G. Anderson, A. E. Dessler, F. N. Keutsch, J. R. Spackman, W. G.

- 476 Read, and T. P. Bui (2007), Observations of deep convective influence on stratospheric  
477 water vapor and its isotopic composition, *Geophysical Research Letters*, *34*(4), L04,814.
- 478 Holton, J. R., and A. Gettelman (2001), Horizontal transport and the dehydration of the  
479 stratosphere, *Geophysical Research Letters*, *28*, 2799–2802.
- 480 Holton, J. R., P. H. Haynes, M. E. McIntyre, A. R. Douglass, R. B. Rood, and L. Pfister  
481 (1995), Stratosphere-troposphere exchange, *Reviews Of Geophysics*, *33*, 403–439.
- 482 James, R., and B. Legras (2009), Mixing processes and exchanges in the tropical and the  
483 subtropical UT/LS, *Atmospheric Chemistry and Physics*, *9*(1), 25–38.
- 484 Johnson, D. G., K. W. Jucks, W. A. Traub, and K. V. Chance (2001), Isotopic compo-  
485 sition of stratospheric water vapor: Implications for transport, *Journal Of Geophysical*  
486 *Research-Atmospheres*, *106*, 12,219–12,226.
- 487 Jouzel, J., L. Merlivat, and B. Federer (1985), Isotopic study of hail - the delta-d-delta-  
488 o-18 relationship and the growth history of large hailstones, *Quarterly Journal Of The*  
489 *Royal Meteorological Society*, *111*, 495–516.
- 490 Keith, D. (2000), Stratosphere-troposphere exchange: Inferences from the isotopic compo-  
491 sition of water vapor, *Journal of Geophysical Research-Atmospheres*, *105*(D12), 15,167  
492 – 15,173.
- 493 Kelly, K. K., M. H. Proffitt, K. R. Chan, M. Loewenstein, J. R. Podolske, S. E. Stra-  
494 han, J. C. Wilson, and D. Kley (1993), Water-vapor and cloud water measurements  
495 over darwin during the step 1987 tropical mission, *Journal Of Geophysical Research-*  
496 *Atmospheres*, *98*, 8713–8723.
- 497 Kirk-Davidoff, D. B., E. J. Hints, J. G. Anderson, and D. W. Keith (1999), The effect  
498 of climate change on ozone depletion through changes in stratospheric water vapour,

- 499 *Nature*, 402, 399–401.
- 500 Kuang, Z., G. Toon, P. Wennberg, and Y. Yung (2003), Measured HDO/H<sub>2</sub>O ratios across  
501 the tropical tropopause, *Geophysical Research Letters*, 30(7).
- 502 Minschwaner, K., and A. E. Dessler (2004), Water vapor feedback in the tropical upper  
503 troposphere: Model results and observations, *Journal Of Climate*, 17, 1272–1282.
- 504 Moyer, E., F. Irion, Y. Yung, and M. Gunson (1996), ATMOS stratospheric deuterated  
505 water and implications for troposphere-stratosphere transport, *Geophysical Research*  
506 *Letters*, 23(17), 2385 – 2388.
- 507 Pfister, L., K. R. Chan, T. P. Bui, S. Bowen, M. Legg, B. Gary, K. Kelly, M. Proffitt,  
508 and W. Starr (1993), Gravity-waves generated by a tropical cyclone during the step  
509 tropical field program - a case-study, *Journal Of Geophysical Research-Atmospheres*,  
510 98, 8611–8638.
- 511 Pfister, L., H. B. Selkirk, E. J. Jensen, M. R. Schoeberl, O. B. Toon, E. V. Browell, W. B.  
512 Grant, B. Gary, M. J. Mahoney, T. V. Bui, and E. Hintsas (2001), Aircraft observations  
513 of thin cirrus clouds near the tropical tropopause, *Journal Of Geophysical Research-*  
514 *Atmospheres*, 106, 9765–9786.
- 515 Pollock, W., L. E. Heidt, R. Lueb, and D. H. Ehhalt (1980), Measurement of strato-  
516 spheric water-vapor by cryogenic collection, *Journal Of Geophysical Research-Oceans*  
517 *And Atmospheres*, 85, 5555–5568.
- 518 Rosenfield, J. E. (1991), A simple parameterization of ozone infrared-absorption for at-  
519 mospheric heating rate calculations, *Journal Of Geophysical Research-Atmospheres*, 96,  
520 9065–9074.

- 521 Sayres, D. S., E. J. Moyer, T. F. Hanisco, J. M. Clair, F. N. Keutsch, A. O'Brien, N. T.  
522 Allen, L. Lapson, J. N. Demusz, M. Rivero, T. Martin, M. Greenberg, C. Tuozzolo,  
523 G. S. Engel, J. H. Kroll, J. B. Paul, and J. G. Anderson (2009), A new cavity based  
524 absorption instrument for detection of water isotopologues in the upper troposphere  
525 and lower stratosphere, *Review Of Scientific Instruments*, 80.
- 526 Schoeberl, M., and L. C. Sparling (1995), Trajectory modelling, diagnostic tools in atmo-  
527 spheric science, *Proc. Int. School of Phys.*, pp. 289–305.
- 528 Smith, C. A., J. D. Haigh, and R. Toumi (2001), Radiative forcing due to trends in  
529 stratospheric water vapour, *Geophysical Research Letters*, 28, 179–182.
- 530 St. Clair, J. M., T. F. Hanisco, E. M. Weinstock, E. J. Moyer, D. S. Sayres, F. N. Keutsch,  
531 J. H. Kroll, J. N. Demusz, N. T. Allen, J. B. Smith, J. R. Spackman, and J. G. Anderson  
532 (2008), A new photolysis laser induced fluorescence technique for the detection of HDO  
533 and H<sub>2</sub>O in the lower stratosphere, *Review of Scientific Instruments*, 79(6).
- 534 Weinstock, E. M., E. J. Hintsa, A. E. Dessler, J. F. Oliver, N. L. Hazen, J. N. Demusz,  
535 N. T. Allen, L. B. Lapson, and J. G. Anderson (1994), New fast-response photofrag-  
536 ment fluorescence hygrometer for use on the nasa er-2 and the perseus remotely piloted  
537 aircraft, *Review Of Scientific Instruments*, 65, 3544–3554.
- 538 Yang, Q., Q. Fu, and Y. Hu (2009), Radiative impacts of clouds in the tropical tropopause  
539 layer, *J. Geophys. Res.*, submitted.

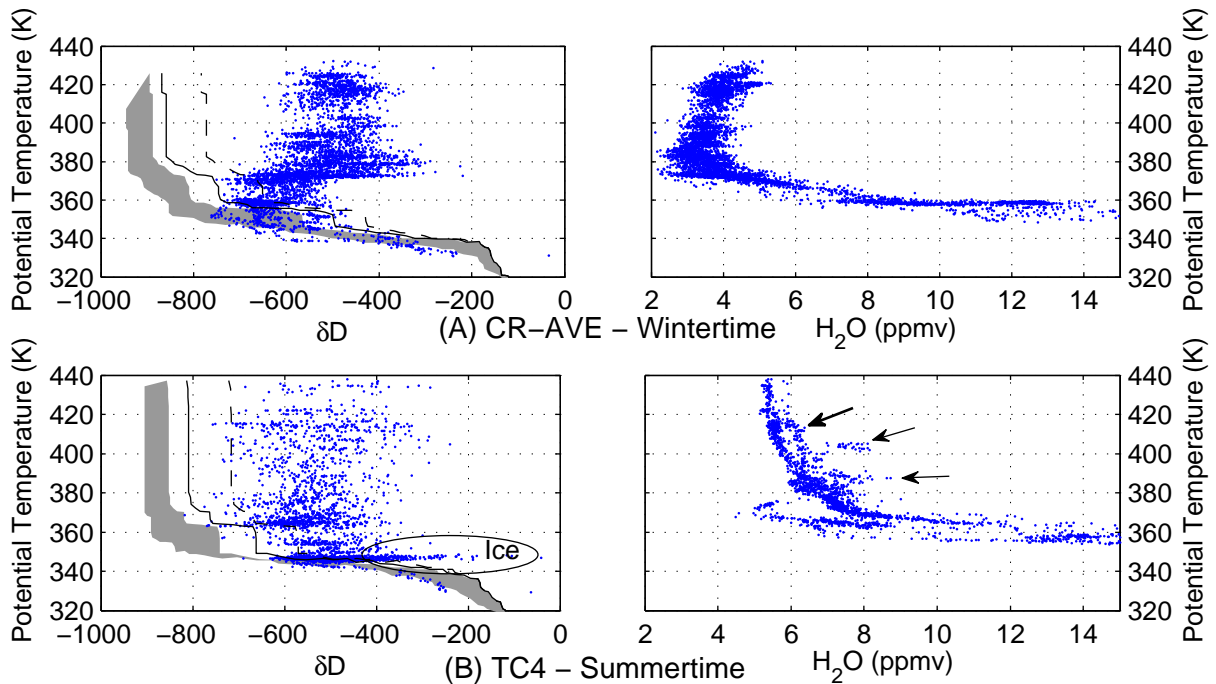


**Figure 1.** Profiles of  $\delta D$  (left) and water vapor mixing ratio (right) versus potential temperature for flights during CR-AVE (A) and TC4 (B). Only data from tropical flights are shown. For the plots of  $\delta D$  the shaded region represents the range of values from a Rayleigh distillation model. The Rayleigh curve plotted here is based on minimum and maximum temperature profiles during each campaign and bounded on the left by an ideal curve where vapor condenses at 100% relative humidity and the condensate is immediately removed and on the right by a curve that includes the effect of 80% condensate retention as the air parcel rises. The shift in the Rayleigh curve due to condensation under supersaturated conditions are shown as solid and dashed black lines for relative humidity of 120% and 150%, respectively. Note that the increased scatter in the summertime data is due to the difference in precision between ICOS and Hoxotope.

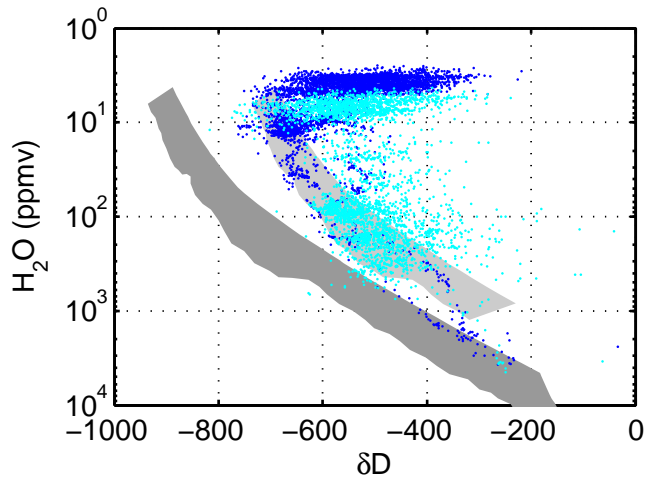


**Figure 2.** Plot of  $\delta D$  versus water vapor with CR-AVE and TC4 data shown in blue and cyan, respectively. The shaded regions represent Rayleigh curves (as in Figure 1) with the light-gray curve shifted by 200‰ from the dark-gray curve at the base of the TTL.

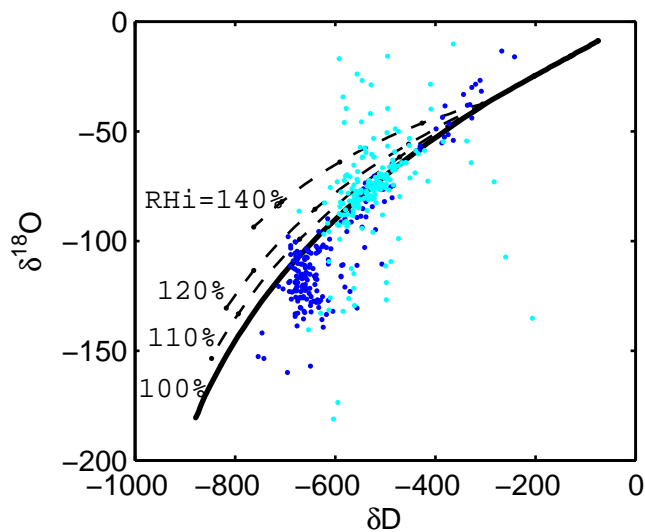


**Figure 3.** Plot of  $\delta^{18}\text{O}$  versus  $\delta D$ . Data from CR-AVE and TC4 are plotted in blue and cyan, respectively. Thick black curve represents the meteoric water line with the dashed curves showing the effect of supersaturation on the relationship between  $\delta^{18}\text{O}$  and  $\delta D$ . Points below the meteoric water line result from mixing of air parcels with different  $\delta$  values.

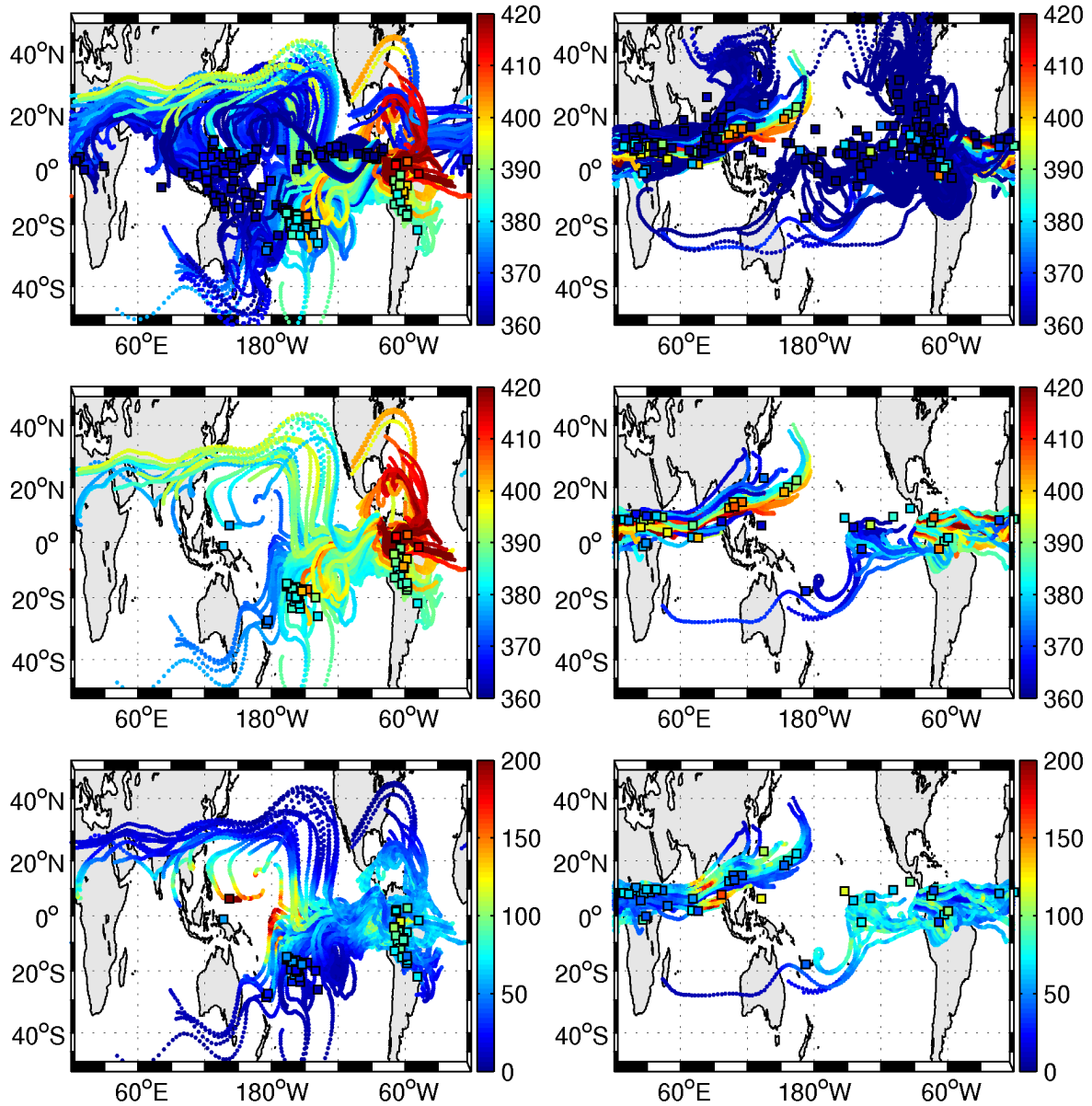


**Figure 4.** Plots show back-trajectories for aircraft flights during the CR-AVE (left plots) and TC4 (right plots) missions. Top (*A* and *B*): Shown are all trajectories that end above the 355 K isentropes and are color coded by potential temperature as given by the colorbar to the right of each plot. Also shown are points along the trajectory where the air was influenced by convection. The mean latitude and longitude of the convection are plotted as black squares color coded by the potential temperature of the trajectory that intersected each convective event. Middle (*C* and *D*): Same as top but for trajectories ending above 380 K. Bottom (*E* and *F*): Same as middle but trajectories are color coded by pseudo relative humidity as described in the text.

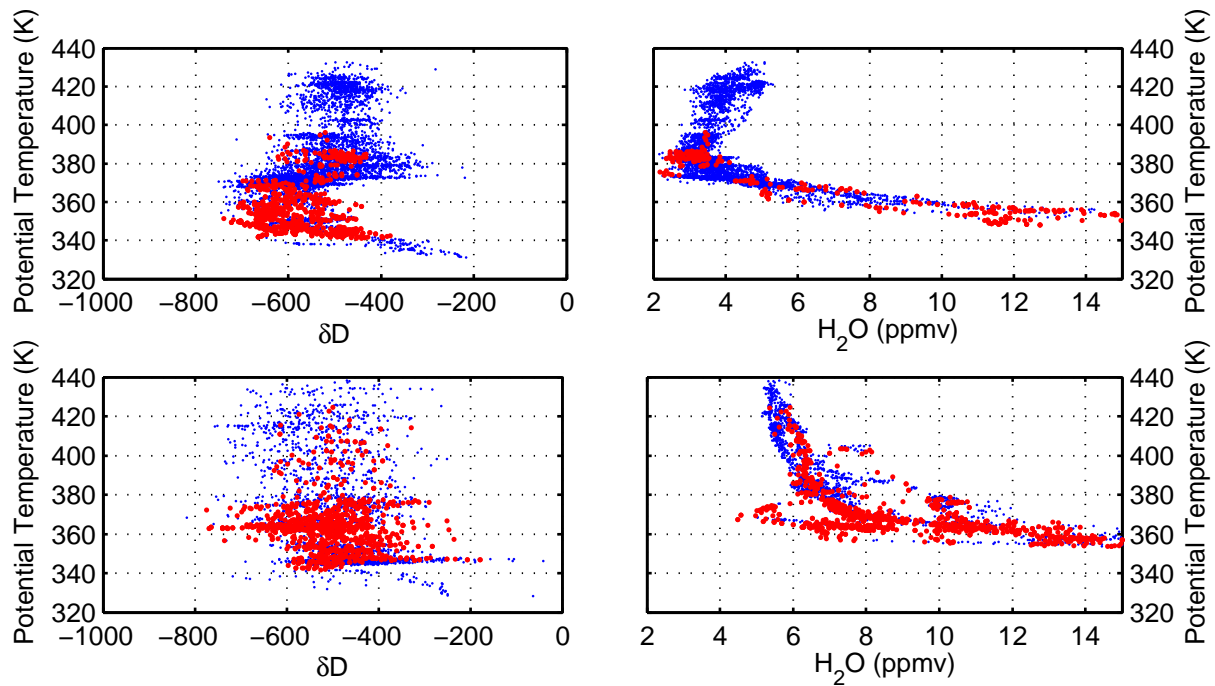


**Figure 5.** Same as Figure 1 with profiles of  $\delta D$  and water vapor mixing ratio plotted versus potential temperature for flights during the CR-AVE (top plots) and TC4 (bottom plots) missions. Data that are convectively influenced, using the criterion that more than 50% of cluster BTs intersect convection and that pseudo-relative humidity at the point of intersection is less than 80%, are highlighted in red.

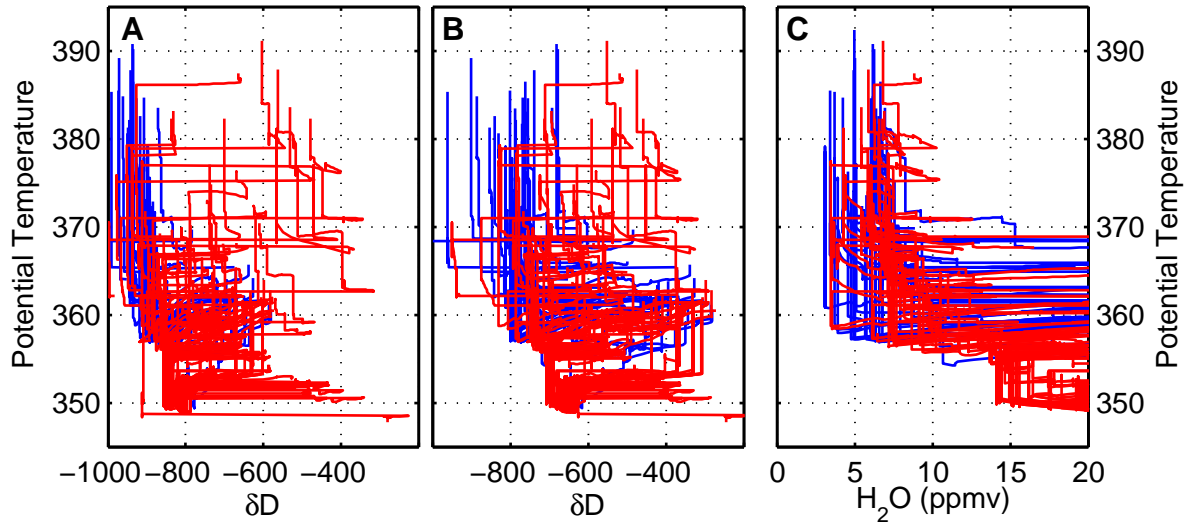


**Figure 6.** Model results of tracking the water vapor mixing ratio and  $\delta D$  of air parcels as they move along diabatic trajectories from TC4 that start between 350 and 360 K.  $\delta D$  (plots *A* and *B*) and water vapor (plot *C*) are plotted versus potential temperature, with trajectories that were influenced by convection plotted in red. Model assumes that parcels are dehydrated to the saturation mixing ratio and trajectories that intersect convection during an unsaturated period are hydrated to a saturation of 100% with ice that has a  $\delta D$  of -100‰. Plot *B* assumes trajectories start with  $\delta D$  enriched by 200‰ as compared to plot *A*. Each line represents a single trajectory starting between 350 and 360 K, with water vapor mixing ratio equal to tens of ppmv and typical  $\delta D$  values of between -400‰ and -600‰.